



HAL
open science

Mobility Analysis of a Large Deployable Reflector Antenna

Philip Long, Stéphane Caro, Juan Reveles, Vincent Fraux, Mike Lawton

► **To cite this version:**

Philip Long, Stéphane Caro, Juan Reveles, Vincent Fraux, Mike Lawton. Mobility Analysis of a Large Deployable Reflector Antenna. Mobility Analysis and Kinematic Performance of OSS Reflector Deployable Structure, Nov 2016, Oxford, United Kingdom. hal-02947118

HAL Id: hal-02947118

<https://hal.science/hal-02947118v1>

Submitted on 23 Sep 2020

HAL is a multi-disciplinary open access archive for the deposit and dissemination of scientific research documents, whether they are published or not. The documents may come from teaching and research institutions in France or abroad, or from public or private research centers.

L'archive ouverte pluridisciplinaire **HAL**, est destinée au dépôt et à la diffusion de documents scientifiques de niveau recherche, publiés ou non, émanant des établissements d'enseignement et de recherche français ou étrangers, des laboratoires publics ou privés.

MOBILITY ANALYSIS OF A LARGE DEPLOYABLE REFLECTOR ANTENNA

Philip Long¹, Stephane Caro², Juan Reveles³, Vincent Fraux³, and Mike Lawton³

¹*IRT Jules Verne, Chemin du Chaffault, 44340 Bouguenais, France*

²*CNRS, IRCCyN, 1 rue de la No, 44321 Nantes, France*

³*Oxford Space Systems, Harwell Space Cluster, Harwell OX11 0QR, UK*

ABSTRACT

Large deployable reflector antennas are complex closed chain systems which are capable of significantly altering their size by modifying configuration space variables. The kinematic analysis of such mechanisms is essential to understanding their behavior during deployment and aid the synthesis of new design as well as establishing the mobility of the system and the most efficient actuation configurations. In this paper, we analyze one facet of a large scale deployable antenna, which during deployment undergoes a *homothetic transformation*. The geometric properties are analyzed under assembly conditions. Furthermore, we show by using screw theory that such a mechanism is feasible and the nature of the motion is demonstrated.

Key words: Screw theory; Kinematic Analysis; Deployable antennas.

1. INTRODUCTION

Deployable mechanisms [Pel14] are complex closed chain systems which are capable of significantly altering their size by modifying configuration space variables. The kinematic analysis of such mechanisms is essential to understanding their behavior during deployment and aid in the synthesis of closed chain structures [RCGR14, DJ99]. Moreover by studying the system's structure, the relationship between input and output variables can be derived which in turn leads to a more informed choice of actuation scheme.

Several methods, which can be broadly divided into numeric and non-numeric methods [LON14], exist to analyze these closed kinematic chains. Numeric methods are typically based on the calculation of the Jacobian matrices [NC15] at each configuration which leads to the creation of closed loop kinematic constraint equations. The Jacobian matrices can be analyzed using advanced algebraic techniques [AMC⁺12a, ACWK12] to identify singularities [AMC⁺12b].

The principal drawback is the complexity which in-

creases with the number of configuration space variables and resulting lack of generality. In addition to this, a physical interpretation of the results is difficult.

On the other hand, non-numeric methods are attractive due to their inherent simplicity [Gog07]. The Chebychev-Grubler-Kutzbach method can be used to calculate the mobility of the closed chain from the number of joints and independent constraint equations, however this system fails for a number of mechanisms. Alternatively, Gogu's method, obtains mobility by decomposing the mechanism into serial chains and examining the operational space of the resulting manipulators.

In this study, we propose to use screw theory [Hun78, LCK12, LKC15], a geometric tool that is capable of analyzing the instantaneous motion of complex mechanisms. In contrast to numeric methods, singular configurations, mobility and actuation scheme analysis can all be obtained without costly derivation of the constraint Jacobian matrix. By using this system, the kinematic performance and mobility of one section of a complex deployable mechanism is studied.

2. SYSTEM DESCRIPTION

The system in question is a large deployable antenna. The system consists of 12 identical facets. Each facet in turn consists of two planar close chain mechanisms as shown in Fig.1. The first mechanism is known as a *scissors mechanism* or SLE [ZCF09] contains five parallel revolute joints each normal to $x - y$ plane. The second mechanism is also planar and consists of a three parallel revolute joints. The two planes are offset by an angle β .

The scissors mechanism, shown in Fig.4 has five parallel revolute joints and two prismatic joints. The two prismatic joints form an angle α , which is constant during the deployment. The following dimensions must be respected [FLRY13, MLY09].

$$|AE| = |EB| = |CE| = |ED| \quad (1)$$

Furthermore the central revolute joint at E , lies on the bisector of the cone. Thus points A, D lie on a secant of a

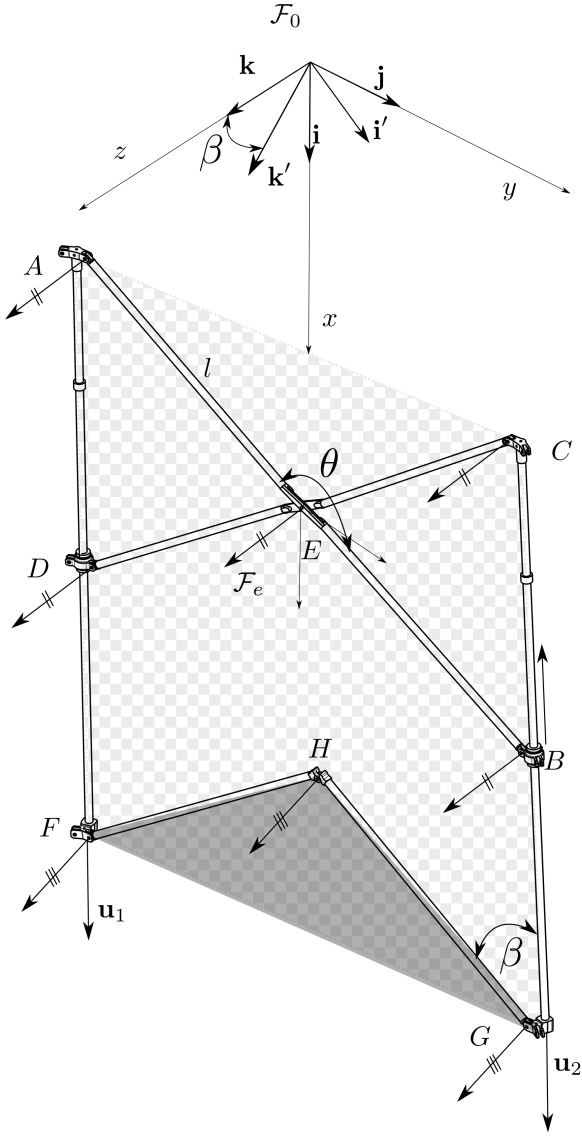


Figure 1. One Facet of deployable mechanism. \mathcal{F}_0 is denoted as fixed world frame. \mathcal{F}_e is denoted as movable end effector frame.

circle centered at E while points C and B lie on a second secant. The angle formed by two secants intersecting outside a circle is given by

$$2\alpha = \frac{\angle DEB - \angle AEC}{2} \quad (2)$$

while since the mechanism is symmetric

$$\angle BEC = \angle DEA \quad (3)$$

thus the following must be hold

$$\theta = \pi - 2\alpha \quad (4)$$

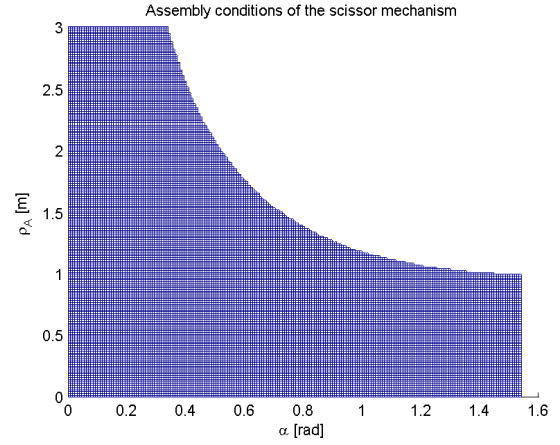


Figure 2. Assembly conditions for a scissors mechanism of $l = 1$. The shaded part of the graph indicates the configuration where the mechanism can be correctly assembled i.e. the center revolute joint of chains AEB and CED coincide.

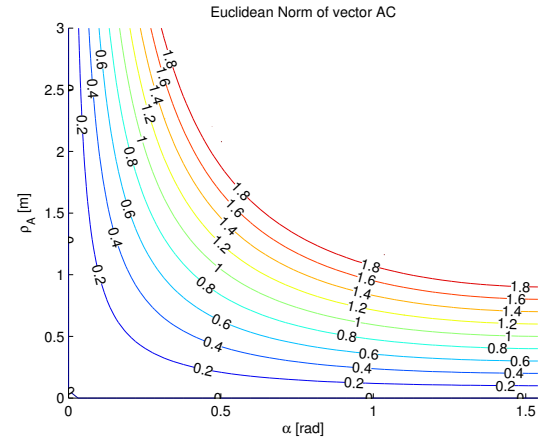


Figure 3. Deployment curves for mechanism when $l = 1$ meter. ρ_A is the distance traveled by the actuated prismatic joint measured from the cone's apex o . $|AC|$ varies from 0 to 1.8 where the maximum theoretical value is $2 \times l$ i.e. 2 meters.

2.1. Deployment Conditions

Equations (1- 4) define the assembly conditions of the mechanism as a function of α . It is assumed that l acts as a scaling factor in the deployment and thus can be fixed. In order to deploy the mechanism, a prismatic joint must be actuated and travel a distance of ρ_A meters. Fig. 2 gives a range for ρ_A and cone angle α , for which the mechanism can be assembled.

For the feasible assembly conditions, Fig. 3, gives the distance $|AC|$ a metric by which we can measure the mechanism deployment. For example at $\alpha = 0.5$, the prismatic joint must travel $\rho_a = 0.7m$, in order to deploy the mechanism from $|AC| = 0 \dots 0.8m$.

3. MOBILITY ANALYSIS

A system's degree of freedom (DOF) is defined as the number of independent coordinates necessary to fix all movable parts. For serial mechanisms this analysis is trivial. However for closed chain mechanism there exist several methods each with their respective pro's and cons, for example the Chebychev-Grübler-Kutzbach, or Gogu's Method [Gog07].

In this paper, we propose *screw theory* as a method to analyze mechanism motion type. In the following section, screw theory is recalled and after which we use it to demonstrate that the motion of the deployable mechanism is feasible. In order to so, virtual prismatic joints are created such that the mechanism as a whole can undergo a *homothetic transformation*. Under these conditions, we show that motion at points E and H is possible.

3.1. Screw Theory

Screw theory is a geometric tool that can be employed to analyze the instantaneous motions of closed chain systems [Hun78, Bal00, LKC15]. A screw of pitch λ is written as:

$$\mathcal{S}_\lambda = \begin{bmatrix} \mathbf{s} \\ \mathbf{s} \times \mathbf{r} + \lambda \mathbf{s} \end{bmatrix} \quad (5)$$

where \mathbf{s} is the rotational screw axis and \mathbf{r} is a vector from any point on \mathbf{s} to the origin of the world frame.

A screw of zero pitch is given as:

$$\begin{bmatrix} \mathbf{s} \\ \mathbf{s} \times \mathbf{r} \end{bmatrix} \quad (6)$$

A zero-pitch twist ν_0 corresponds to a pure rotation about axis \mathbf{s} i.e. an instantaneous angular velocity. A zero-pitch wrench ζ_0 corresponds to a pure force along axis \mathbf{s} .

An infinite-pitch screw is given by:

$$\begin{bmatrix} \mathbf{0} \\ \mathbf{s} \end{bmatrix} \quad (7)$$

An infinity-pitch twist ν_∞ corresponds to a pure translation along axis \mathbf{s} i.e. an instantaneous linear velocity. An ∞ -pitch wrench ζ_∞ corresponds to a pure moment about axis \mathbf{s} .

For any set of n linearly independent screws, there exists a reciprocal set of dimension $6 - n$. Reciprocity between screw \mathcal{S}_1 and \mathcal{S}_2 implies that the instantaneous power, given by (8) is zero.

$$\left(\begin{bmatrix} \mathbf{0}_{3 \times 3} & \mathbf{I}_3 \\ \mathbf{I}_3 & \mathbf{0}_{3 \times 3} \end{bmatrix} \mathcal{S}_1 \right)^T \mathcal{S}_2 = 0 \quad (8)$$

The above expression is valid for screws of any pitch, however there are three particularly useful conditions which can be defined from (8):

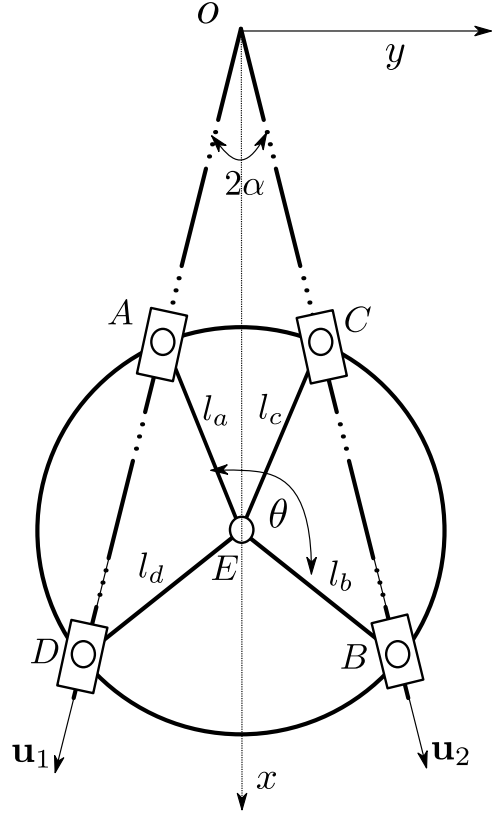


Figure 4. Planar view of scissors mechanism

1. A \mathcal{S}_0 is reciprocal to \mathcal{S}_∞ if their axes are orthogonal;
2. A \mathcal{S}_∞ is always reciprocal to another \mathcal{S}_∞ ;
3. Two \mathcal{S}_0 are reciprocal if their axes are coplanar;

It should be noted that coplanar means either intersecting or parallel.

3.2. Mobility Analysis of Scissors Mechanisms

The facet is analyzed by decomposing the closed chain system into a series of sub-mechanisms. For the scissors type mechanism shown in Fig.4, we follow the method outlined in [CDFX14].

Firstly, the mechanism is divided into two chains, the first chain is defined as linkage AEB , denoted as chain 1, and the second of linkage CED denoted as chain 2. We consider that the mechanism can slide along the cone in a *homothetic transformation*, thus both chains AEB and CED are represented as parallel mechanism with two limbs both of configuration RP, with the terminal frame located at point E . In the following, a mobility analysis is carried out for the first chain i.e., AEB as illustrated in Fig. 5.

The infinite and zero pitch twists associated respectively with the prismatic and revolute joint at point A are given

as:

$$\nu_{\infty 1}^A = \begin{bmatrix} \mathbf{0} \\ \mathbf{u}_1 \end{bmatrix} \quad \nu_{02}^A = \begin{bmatrix} \mathbf{k} \\ \mathbf{k} \times \mathbf{u}_A \end{bmatrix} \quad (9)$$

where \mathbf{u}_1 , \mathbf{u}_A and \mathbf{k} denote the unit vectors along AD , AE and the z -axis respectively.

The twist system at A is a 2-system and is given as $T_A = \text{span}(\nu_{\infty 1}^A, \nu_{02}^A)$. Outside singular configurations, the limb constraint wrench system, denoted as W_A^c , is a 4-system spanned by the following constraint wrenches:

$$\zeta_{\infty 1}^A = \begin{bmatrix} \mathbf{0} \\ \mathbf{i} \end{bmatrix} \quad \zeta_{\infty 2}^A = \begin{bmatrix} \mathbf{0} \\ \mathbf{j} \end{bmatrix} \quad (10)$$

$$\zeta_{03}^A = \begin{bmatrix} \mathbf{k} \\ \mathbf{k} \times \mathbf{u}_a \end{bmatrix} \quad \zeta_{04}^A = \begin{bmatrix} \mathbf{u}_1 \times \mathbf{k} \\ (\mathbf{u}_1 \times \mathbf{k}) \times \mathbf{u}_A \end{bmatrix} \quad (11)$$

Using the reciprocity conditions, $\zeta_{\infty 1}^A$ and $\zeta_{\infty 2}^A$ can be chosen as any two linearly pure moments in the xy plane, for simplicity their axes are chosen as \mathbf{i} and \mathbf{j} which denote the unit vectors parallel to the x and y axes respectively. ζ_{03}^A is a pure force orthogonal to the $x - y$ plane, while ζ_{04}^A is a pure force orthogonal to \mathbf{u}_1 and passing through point A .

The above process is repeated for the second limb of chain 1. Thus the twists associated respectively with the prismatic and revolute joint at point B are given as:

$$\nu_{\infty 1}^B = \begin{bmatrix} \mathbf{0} \\ \mathbf{u}_2 \end{bmatrix} \quad \nu_{02}^B = \begin{bmatrix} \mathbf{k} \\ \mathbf{k} \times \mathbf{u}_B \end{bmatrix} \quad (12)$$

where \mathbf{u}_2 , \mathbf{u}_B and \mathbf{k} denote the unit vectors along CB , BE and the z -axis respectively.

The twist system at B is given as $T_B = \text{span}(\nu_{\infty 1}^B, \nu_{02}^B)$. Outside singular configurations,

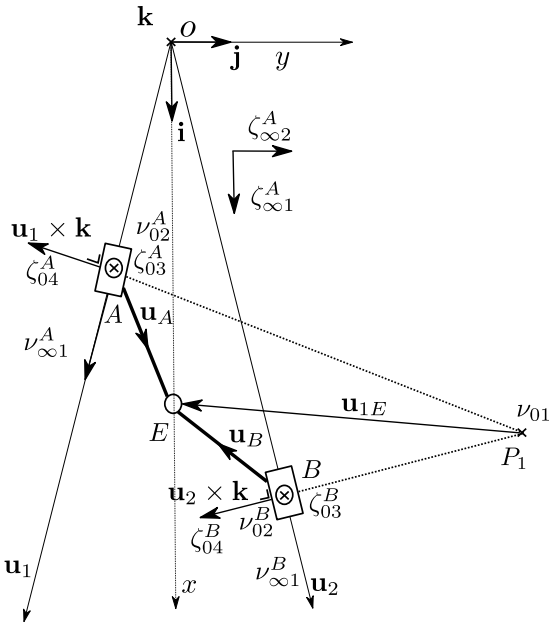


Figure 5. Twists and wrenches associated with chain 1

the limb constraint wrench system, W_B^c , is spanned by:

$$\zeta_{\infty 1}^B = \begin{bmatrix} \mathbf{0} \\ \mathbf{i} \end{bmatrix} \quad \zeta_{\infty 2}^B = \begin{bmatrix} \mathbf{0} \\ \mathbf{j} \end{bmatrix} \quad (13)$$

$$\zeta_{03}^B = \begin{bmatrix} \mathbf{k} \\ \mathbf{k} \times \mathbf{u}_B \end{bmatrix} \quad \zeta_{04}^B = \begin{bmatrix} \mathbf{u}_2 \times \mathbf{k} \\ (\mathbf{u}_2 \times \mathbf{k}) \times \mathbf{u}_B \end{bmatrix} \quad (14)$$

The constraint wrench system of the scissors mechanism is the union of the limb's wrench constraint systems, given as:

$$W^c = \text{span}(W_A^c, W_B^c) \quad (15)$$

after removing linear independent wrenches, the constraint wrench system becomes:

$$W^c = \text{span}(\zeta_{\infty 1}^A, \zeta_{\infty 2}^A, \zeta_{03}^A, \zeta_{03}^B, \zeta_{04}^A, \zeta_{04}^B) \quad (16)$$

In order to find a feasible motion of chain 1, we must find a twist that is reciprocal to the constraint wrench system. Using the reciprocity conditions, it can be seen that a 0-pitch twist parallel to \mathbf{k} is coplanar to ζ_{03}^A and ζ_{03}^B while orthogonal to $\zeta_{\infty 1}^A$ and $\zeta_{\infty 2}^A$. In addition to this, if the twist passes through point P_1 , it is also coplanar to ζ_{04}^A and ζ_{04}^B . Therefore the twist of chain 1 can be written as:

$$\nu_{01} = \begin{bmatrix} \mathbf{k} \\ \mathbf{k} \times \mathbf{u}_{1E} \end{bmatrix} \quad (17)$$

where \mathbf{u}_{1E} is the vector from point P_1 to point E . P_1 is defined by the intersection of a vector with direction $(\mathbf{u}_1 \times \mathbf{k})$ that passes through point A and a vector with direction $(\mathbf{u}_2 \times \mathbf{k})$ that passes through point B . Hence, it can be seen that chain AEB has 1-DOF, defined as a pure rotation around P_1 . Instantaneously at point E , this pure rotation is a linear velocity tangential to a circle with center P_1 and radius $\|EP_1\|$.

The same method is employed to obtain the twist allowable by chain 2, which is written as:

$$\nu_{02} = \begin{bmatrix} \mathbf{k} \\ \mathbf{k} \times \mathbf{u}_{2E} \end{bmatrix} \quad (18)$$

where \mathbf{u}_{2E} is the vector from point P_2 to point E . P_2 is defined by the intersection of a vector with direction $(\mathbf{u}_2 \times \mathbf{k})$ that passes through point C and a vector with direction $(\mathbf{u}_1 \times \mathbf{k})$ that passes through point D . Therefore, similar to AEB , chain CED has 1-DOF, defined as a pure rotation around P_2 . Instantaneously at point E , this pure rotation is a linear velocity tangential to a circle with center P_2 and radius $\|EP_2\|$.

In order for the mechanism to be feasible, ν_{01} and ν_{02} must be linearly dependent. By examination of (17) and (18) it can be seen that to satisfy this condition \mathbf{u}_{1E} and \mathbf{u}_{2E} must be collinear.

$$\frac{\mathbf{u}_{1E} \cdot \mathbf{u}_{2E}}{\|\mathbf{u}_{1E}\| \|\mathbf{u}_{2E}\|} = 1 \quad (19)$$

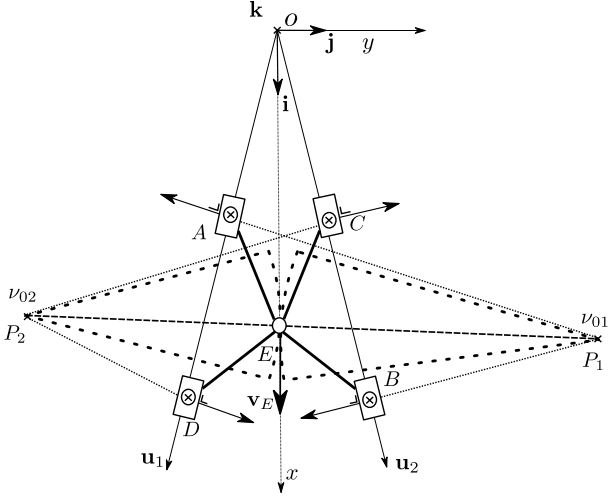


Figure 6. Solution set for instantaneous motion of E . The instantaneous linear velocity of E , \mathbf{v}_E , is shown as the tangent to the circle with center P_2 and radius $\|EP_2\|$

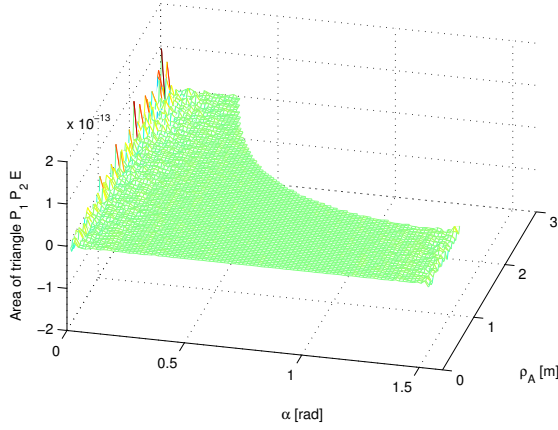


Figure 7. Area of triangle formed by P_1 , P_2 and E plotted for geometric assembly conditions

This means that the point E must lie on the line formed by P_1 and P_2 as shown in Fig.6. To facilitate the presentation, we choose to study the area of the triangle formed by P_1 , P_2 and E . In the case of collinearity, this must be zero i.e.:

$$\det \left(\begin{bmatrix} 1 & P_1 \\ 1 & P_2 \\ 1 & E \end{bmatrix} \right) = 0 \quad (20)$$

From (19) and (20), it can be seen that there are infinite feasible positions of point E along the line formed by points P_1 P_2 . In Fig.7, the area of the triangle given in (20) is plotted for the geometric assembly conditions as shown in Fig.2. It can be seen that within assemble conditions the area of the triangle is zero, thus P_1 , P_2 and E are collinear. It follows that ν_{01} and ν_{02} generate a linear velocity in the same direction and the mechanism is movable.

Finally, It should be noted in the special case where vectors \mathbf{u}_1 and \mathbf{u}_2 are parallel, i.e. $\alpha = 0$, the twist of chain 1, is a pure translation along the x -axis written as:

$$\nu_{\infty 1} = \begin{bmatrix} \mathbf{0} \\ \mathbf{i} \end{bmatrix} \quad (21)$$

3.3. Mobility analysis of Second Mechanism

In order for the facet to deploy, both mechanisms must follow the *homothetic transformation*. In the following section, the second mechanism consisting of points FGH is analyzed to ensure that motion is possible under homothetic conditions.

Similar to one chain of the scissors mechanisms, this mechanism can be represented as a RP-RP closed chain system with the platform located at point H . The infinite and zero pitch twists associated respectively with the prismatic and revolute joint at point F are given as:

$$\nu_{\infty 1}^F = \begin{bmatrix} \mathbf{0} \\ \mathbf{u}_1 \end{bmatrix} \quad \nu_{02}^F = \begin{bmatrix} \mathbf{k}' \\ \mathbf{k}' \times \mathbf{u}_F \end{bmatrix} \quad (22)$$

where

$$\mathbf{k}' = \mathbf{R}(\beta, y) \mathbf{k} \quad (23)$$

\mathbf{u}_F denotes the unit vector along FH and $\mathbf{R}(\beta, y)$ denotes a rotation of β radians around the y axis.

The limb constraint wrench system, denoted as \mathcal{W}_F^c , is a 4-system spanned by the following constraint wrenches:

$$\zeta_{\infty 1}^F = \begin{bmatrix} \mathbf{0} \\ \mathbf{i}' \end{bmatrix} \quad \zeta_{\infty 2}^F = \begin{bmatrix} \mathbf{0} \\ \mathbf{j} \end{bmatrix} \quad (24)$$

$$\zeta_{03}^F = \begin{bmatrix} \mathbf{k} \\ \mathbf{k} \times \mathbf{u}_f \end{bmatrix} \quad \zeta_{04}^F = \begin{bmatrix} \mathbf{u}_1 \times \mathbf{k} \\ (\mathbf{u}_1 \times \mathbf{k}) \times \mathbf{u}_F \end{bmatrix} \quad (25)$$

Using the reciprocity conditions, $\zeta_{\infty 1}^F$ and $\zeta_{\infty 2}^F$ can be chosen as any two linearly pure moments in the rotated $x - y$ plane, for simplicity their axes are chosen as \mathbf{i}' and \mathbf{j} , where \mathbf{i}' denotes the \mathbf{i} vector rotated β radians around the y axis. ζ_{03}^F is a pure force orthogonal to the xy plane and passing through point F , while ζ_{04}^F is a pure force orthogonal to \mathbf{u}_1 and passing through point F .

The above process is repeated for the second limb of chain. Thus the twists associated respectively with the prismatic and revolute joint at point G are given as:

$$\nu_{\infty 1}^G = \begin{bmatrix} \mathbf{0} \\ \mathbf{u}_2 \end{bmatrix} \quad \nu_{02}^G = \begin{bmatrix} \mathbf{k}' \\ \mathbf{k}' \times \mathbf{u}_G \end{bmatrix} \quad (26)$$

where \mathbf{u}_G denotes the unit vector along GH .

Outside singular configurations, the limb constraint wrench system, \mathcal{W}_G^c , is spanned by:

$$\zeta_{\infty 1}^G = \begin{bmatrix} \mathbf{0} \\ \mathbf{i}' \end{bmatrix} \quad \zeta_{\infty 2}^G = \begin{bmatrix} \mathbf{0} \\ \mathbf{j} \end{bmatrix} \quad (27)$$

$$\zeta_{03}^G = \begin{bmatrix} \mathbf{k} \\ \mathbf{k} \times \mathbf{u}_g \end{bmatrix} \quad \zeta_{04}^G = \begin{bmatrix} \mathbf{u}_2 \times \mathbf{k} \\ (\mathbf{u}_2 \times \mathbf{k}) \times \mathbf{u}_G \end{bmatrix} \quad (28)$$

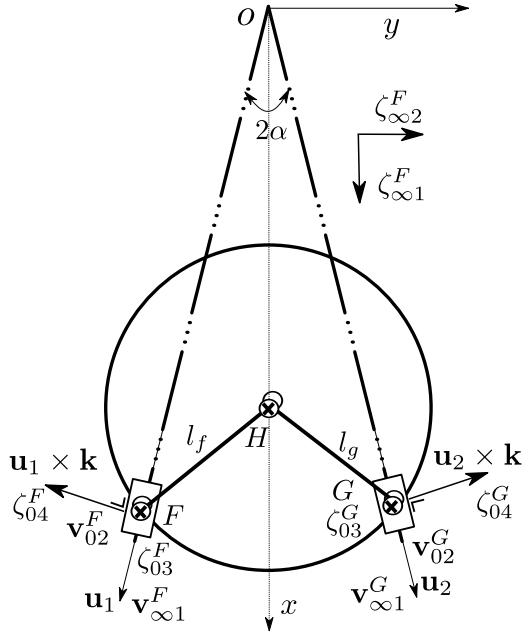


Figure 8. Twists and wrenches associated with second sub-mechanism

The constraint wrench system of the sub-mechanism is the union of the each limb's wrench system, given as:

$$W^c = \text{span} (W_F^c \quad W_G^c) \quad (29)$$

after removing linear independent wrenches becomes:

$$W^c = \text{span} (\zeta_{\infty 1}^F \quad \zeta_{\infty 2}^F \quad \zeta_{03}^F \quad \zeta_{04}^F \quad \zeta_{03}^G \quad \zeta_{04}^G) \quad (30)$$

In order to find a feasible motion of point H , we must find a twist that is reciprocal to the constraint wrench system. Unlike the scissors mechanism from Section 3.2, there are no zero nor infinity pitch reciprocal the system. However, it can be shown that outside singular configurations $\text{rank}(W^c) = 5$, thus the twist system is of order 1 and motion is possible under a *homothetic transformation conditions*

4. CONCLUSION

In this study we analyzed one facet of a large scale deployable reflector antenna. Firstly, we have shown how the deployment properties are dependent on the geometric conditions of the mechanism. Secondly, screw theory was used to demonstrate that motion is possible under *homothetic transformation conditions*. In addition to this, the type of motion and constraint applied by each sub-mechanism were illustrated. Future work will focus on an actuation scheme analysis to obtain the optimum actuator performance for deployment.

REFERENCES

- [ACWK12] Semaan Amine, Stéphane Caro, Philippe Wenger, and Daniel Kanaan. Singularity analysis of the h4 robot using grassmann–cayley algebra. *Robotica*, 30(07):1109–1118, 2012.
- [AMC⁺12a] Semaan Amine, Mehdi Tale Masouleh, Stéphane Caro, Philippe Wenger, and Clément Gosselin. Singularity analysis of 3t2r parallel mechanisms using grassmann–cayley algebra and grassmann geometry. *Mechanism and Machine Theory*, 52:326–340, 2012.
- [AMC⁺12b] Semaan Amine, Mehdi Tale Masouleh, Stéphane Caro, Philippe Wenger, and Clément Gosselin. Singularity conditions of 3t1r parallel manipulators with identical limb structures. *Journal of Mechanisms and Robotics*, 4(1):011011, 2012.
- [Bal00] S. R.S Ball. *A Treatise on the Theory of Screws*. Cambridge Univ Pr, 1900.
- [CDFX14] Jianguo Cai, Xiaowei Deng, Jian Feng, and Yixiang Xu. Mobility analysis of generalized angulated scissor-like elements with the reciprocal screw theory. *Mechanism and Machine Theory*, 82:256–265, 2014.
- [DJ99] Jian S Dai and J Rees Jones. Mobility in metamorphic mechanisms of foldable/erectable kinds. *Journal of mechanical design*, 121(3):375–382, 1999.
- [FLRY13] V Fraux, M Lawton, JR Reveles, and Z You. Novel large deployable antenna backing structure concepts for foldable reflectors. *CEAS Space Journal*, 5(3-4):195–201, 2013.
- [Gog07] G. Gogu. *Structural Synthesis of Parallel Robots: Part 1: Methodology*. Springer Verlag, 2007.
- [Hun78] K. Hunt. *Kinematic geometry of mechanisms*. Cambridge Univ Press, 1978.
- [LCK12] Philip Long, Stéphane Caro, and Wisama Khalil. Kinematic analysis of lower mobility cooperative arms by screw theory. In *9th International Conference on Informatics in Control Automation and Robotics*, pages 208–285, 2012.
- [LKC15] Philip Long, Wisama Khalil, and Stéphane Caro. Kinematic and dynamic analysis of lower-mobility cooperative arms. *Robotica*, 33(09):1813–1834, 2015.
- [LON14] Philip LONG. *Contributions to the Modeling and Control of Cooperative Manipulators*. PhD thesis, Ecole Centrale de Nantes, 2014.
- [MLY09] Decan Mao, Yaozhi Luo, and Zhong You. Planar closed loop double chain linkages. *Mechanism and Machine Theory*, 44(4):850–859, 2009.

- [NC15] Latifa Nurahmi and Stéphane Caro. Dimensionally homogeneous extended jacobian and condition number. In *2nd International Conference on Mechanical Engineering (ICOME 2015)*, 2015.
- [Pel14] Sergio Pellegrino. *Deployable structures*, volume 412. Springer, 2014.
- [RCGR14] Lennart Rubbert, Stéphane Caro, Jacques Gangloff, and Pierre Renaud. Using singularities of parallel manipulators to enhance the rigid-body replacement design method of compliant mechanisms. *Journal of Mechanical Design*, 136(5):051010, 2014.
- [ZCF09] Jing-Shan Zhao, Fulei Chu, and Zhi-Jing Feng. The mechanism theory and application of deployable structures based on sle. *Mechanism and Machine Theory*, 44(2):324–335, 2009.